ORIGINAL ARTICLE

Hydrogeochemical modeling and dedolomitization processes in the Patagonian Boulders and Patagonia Formation in the eastern Patagonia, Argentina

Guilermo Osvaldo Baumann[1] · Melanie Vital[2,3] · Melisa Glok-Galli[4] · Sebastián Grondona[2,3] · Héctor Massone[2] · Daniel Emilio Martinez[2,3]

Abstract

The aim of this study was to contribute to the understanding of the hydrogeological system of the Argentine Patagonia Extra-Andina region, focused on the Atlantic coastal area at 46° south latitude. The hydrogeochemical aspects of this aquifer system were taken into consideration for this purpose. The database includes 193 chemical analyses of major ions obtained through standard laboratory methods. A statistical analysis of the data, as well as the realization of hydrochemical models using PHREEQC software, was performed. The regional groundwater flows from west to east, with the recharge water being a sodium–chloride–bicarbonate type, and the discharge of water is typified as a sodium–sulfate–chloride type. The hydrogeochemical evolution of the aquifer shows a general augmentation of salinity and major ions in the groundwater-flow path, except for HCO_3^-. Inverse hydrochemical modeling showed that gypsum dissolution with calcite precipitation, Ca^{2+}/Na^+ and Mg^{2+}/Na^+ ionic exchange, and dedolomitization are the main processes along the groundwater flow pathway.

Keywords Eastern patagonia · Dedolomitization · Hydrogeochemical modeling · Patagonic boulders

Introduction

Patagonia is a geographical region located in the southern part of South America. It is divided into a western area called Patagonia Andina, characterized by the presence of the Andes Mountains, with elevations up to 3776 m (Lanín Volcano). The eastern area known as Patagonia Extra-Andina is an area of low altitude plateaus with a low regional slope, ranging from 0.015 to 0.03%, towards the Atlantic Ocean. Both sectors differ significantly in terms of their climate. In the Andean region, because of the presence of a highly elevated landscape, the humidity from the Pacific Ocean is retained, and

rain fall reaches up to 2000 mm/year, leading to the formation of a phytogeographic region known as the Valdivian Forest.

On the opposite side of the highlands, the Extra-Andina region in contrast has a predominance of dry weather and the water balance performed in this sector indicates a deficit of 1200 mm/year (Hernández et al. 2008). These climatic conditions make groundwater in this area the only source of water for productive activities and for urban supply. The most important cities in the region are Comodoro Rivadavia (200,000 inhabitants), in the Chubut Province, and Caleta Olivia (70,000 inhabitants) in the Santa Cruz Province (Fig. 1). The control of groundwater exploitation is important to prevent the depletion of the aquifers. The lack of water is an issue that afflicts the entire population of Caleta Olivia. Water shortages occur very frequently over the years, for example, in the year 2010, there were 84 water shortages (Boix and Gigli 2010). Moreover, the study area is heavily impacted by oil extraction because it is located in the oil exploitation area known as "San Jorge Gulf Basin" (the oldest and most productive in Argentina with 42% of the national production). The San Jorge Gulf Basin includes oil-bearing strata which have led to the development of an exploitation area. The most important oil source rocks of

✉ Daniel Emilio Martinez
  demarti@mdp.edu.ar

[1] Servicios Públicos S.E. Prov. De Santa Cruz, Santa Cruz, Argentina

[2] Instituto de Geología de Costas y del Cuaternario, UNMDP-CICPBA, Mar del Plata, Argentina

[3] Instituto de Investigaciones Marinas y Costeras, CONICET-UNMDP, Mar del Plata, Argentina

[4] INMAT (UNCPBA)-CIFICEN (UNCPBA-CICPBA-CONICET), Mar del Plata, Argentina
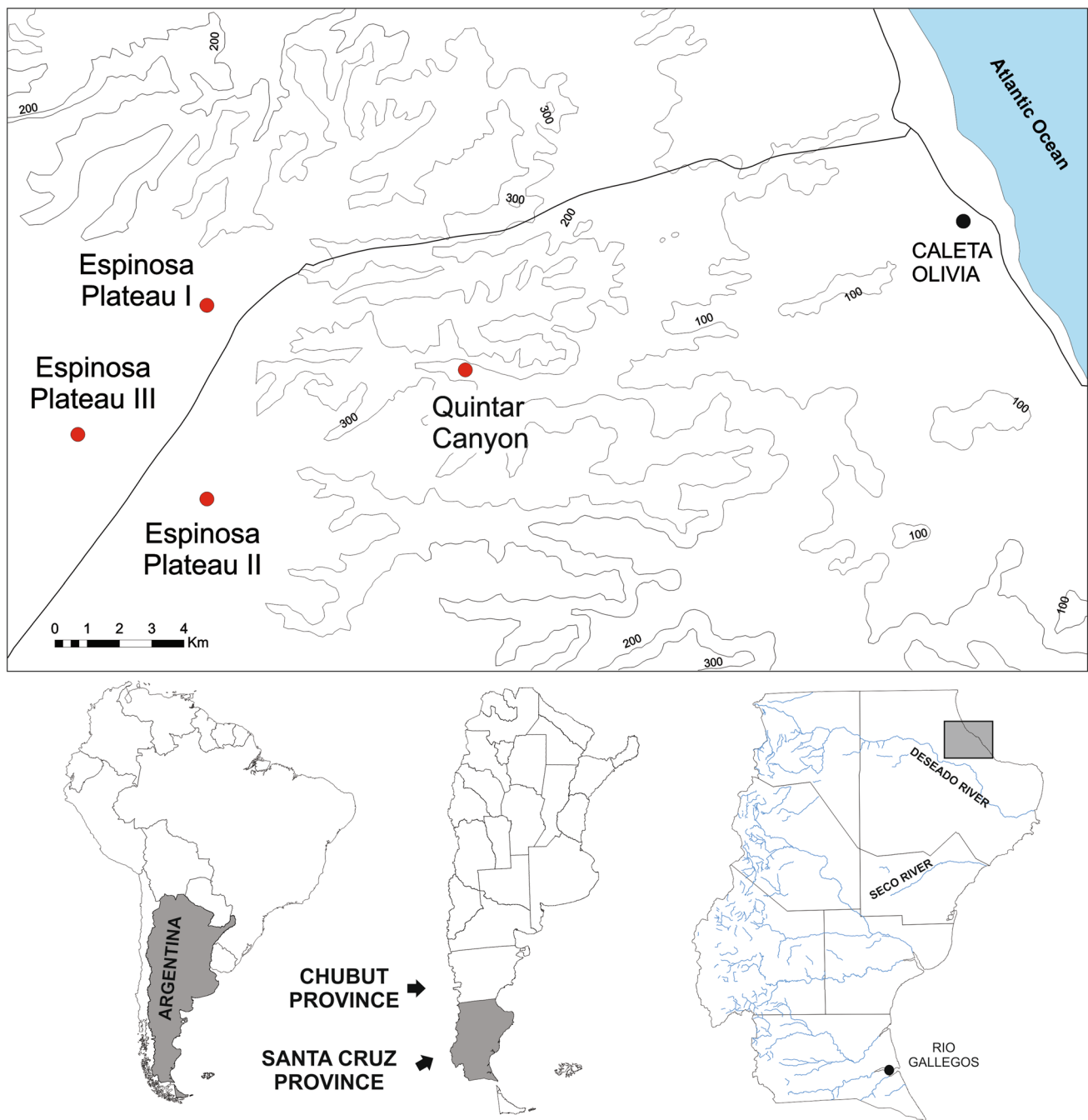
Fig. 1 Location map (1: Chubut Province, 2: Neuquén Province)

the basin belong to the Lower Cretaceous at a depth of over 5000 m (Sylwan 2001), but their exploitation is a threat for shallow groundwater resources because of the discharge of the formation water in surface. The upstream oil and gas activities are internationally recognized as high risk for groundwater environmental safety (WWAP 2015) because of the accumulation of total dissolved solids after formation waters were discharged on to the surface. The formation water usually is a brine with a substantial concentration of ionizing molecules, such as sodium chloride and potassium chloride, and its accumulation on land is considered a potential pollution source.

The hydrogeochemical aspects of the aquifer system in the region of Caleta Olivia, Province of Santa Cruz, Argentine Patagonia, are considered in this work, to contribute to the understanding of the hydrogeological system. A better knowledge of aquifer characteristics will allow designing improved and more effective management instruments as

a way to preserve groundwater quantity and quality. The study is specifically focused on an area located 35 km from the city of Caleta Olivia, corresponding to the Espinosa Plateau (EP) and Quintar Canyon (QC) (Fig. 1), where the exploitation wells that supply water to the entire town are located. The city of Caleta Olivia has about 70,000 inhabitants and its economy is based on the oil exploitation in the surrounding area. Moreover, two exploratory wells for gas prospecting were authorized in 2018, and the concern about water-resource protection is increasing in the local population. The use of existing hydrochemical information applying hydrogeochemical modeling can aid in increasing the knowledge of the hydrogeological systems and, thus, can provide basic information for water-supply protection and management.

Climate

The main climatic features have been previously characterized by Auge et al. (2010) on the basis of records from the meteorological station at the Comodoro Rivadavia Airport, belonging to the NMS (National Weather Survey), located approximately 90 km to the north of the Caleta Olivia (Fig. 1). Considering a range of 10 years within the period 1941–2000, the average annual values of precipitation and temperature registered were 247.5 mm and 12–13 °C, respectively. During the coldest months (fall and winter), the most precipitation has historically been recorded (approximately 65% of the total), while the lowest precipitation (35% remaining) was recorded in the warmer months (spring and summer). The temperature is the highest in January, with the average maximum being between 25 and 26 °C. For the month of July, the average minimum values are about 3 °C. Over the same period of time, when the average values of temperature and precipitation are compared, an inversion between the respective maximum and minimum can be observed. Most rainfall occurs in the months of lower temperatures and vice versa.
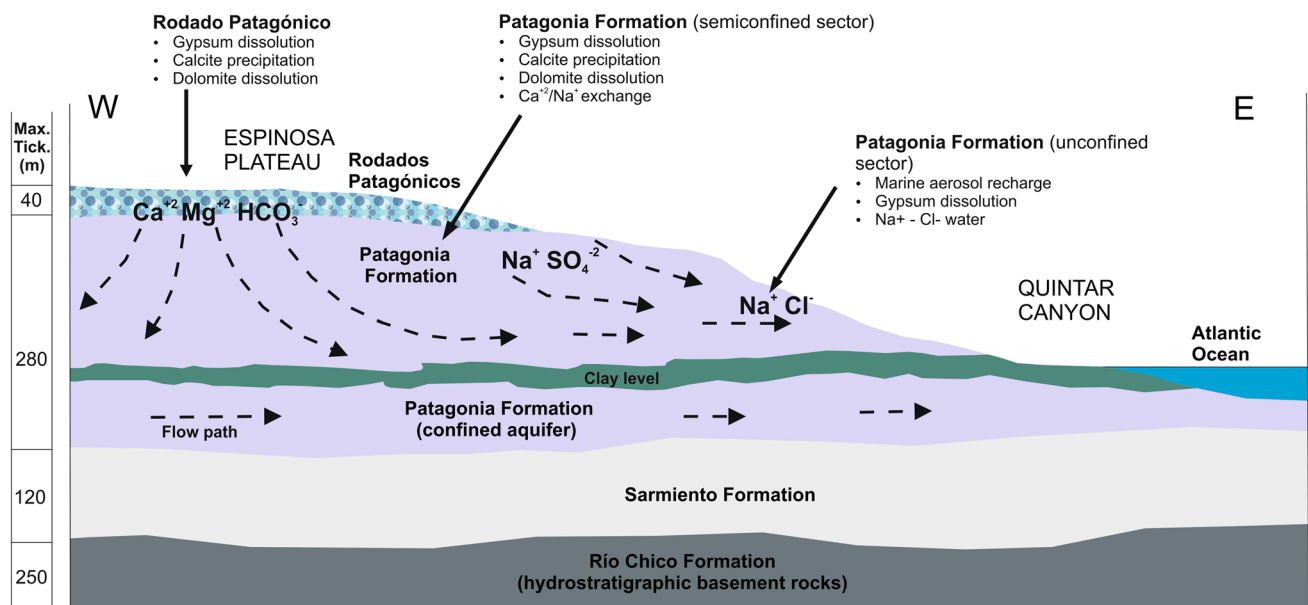
Geology

The total area of the San Jorge Gulf Basin is about 200,000 km^2, of which 65% is on the continent and the rest extends into the sea. Of the total surface area, approximately 70,000 km^2 are of interest to explorationists for oil extraction. The maximum sediment thickness is about 7000 m, coinciding with the largest embayment within the continent (Sylwan 2001), approximately along the border between Chubut and Santa Cruz Provinces (Fig. 1). In the study area, the oldest rocks consist of sedimentary, igneous and metamorphic rocks, dating from the Cambrian to Devonian in age, which were part of the Nord Patagonian and Deseado Cratons before the extensional origin of the

basin in the Upper Jurassic. The Bahía Laura Group (de Barrio et al. 1999), dating from the Middle to Upper Jurassic and comprising the Chon Aike formational units (ignimbrites, tuffs, breccias, agglomerates, lavas and subvolcanic), overlaps the La Matilde Formation (deposits of tuff and tuffites interdigitated with interspersed ignimbrites).

From the Upper Jurassic and until the Lower Cretaceous, mudstones of the Well D-129 Formation (Lesta 1968) were deposited. This unit is the unique sequence representative of the Las Heras Group (Lesta and Ferello 1972) and is considered as the main oil source rock in the basin. This is overlying the Chubut Group, which includes the Cañadón Seco and the Mina El Carmen formations (Lesta 1968), which are important because of the presence of interspersed sandy bodies that have provided the largest amount of hydrocarbons extracted from the basin.

Tertiary deposits present include sedimentation initiated in the Lower Paleocene as the marine transgression dominated Salamanca Formation (Lhering 1907). During the Upper Paleocene, an important fluvial cycle deposited the Río Chico Formation (Simpson 1933, 1935) as noted at the base of Fig. 2. It has a layer of plastic clays (montmorillonite) in its uppermost part that makes the unit to behave as the hydrogeological basement or confining layer of the area. In the early Oligocene, tuffs and continental bentonites from the Sarmiento Formation (Feruglio 1949) were deposited (Fig. 2). This deposit can be divided into two sections: a basal unit with tuffs possessing a high degree of consolidation, and atop, formed by cineritic tuffs with a minor degree of consolidation. The upper section has a thickness of 30–40 m, with a gradual wedging into the Deseado River (Fig. 1), outcropping in the modern valley.

Finally, sediments deposited during Oligocene marine transgressions (middle part of Fig. 2) constitute the Patagonia Formation (Zambrano and Urien 1970), which is typified by sand interspersed with traces of bivalves in the upper section, while at the lower section, sandy-clayed grain size becomes dominant. Its thickness reaches its maximum in the north of the area (approximately 150 m thick), gradually wedges toward the south, to 130 m in thickness in the Astra area (45°44′00″S, 67°30′00″W), to 60 m in the Cordon region, and to less than 10 m in the city of Pico Truncado (46°48′00″S, 67°58′00″W). Unconformably overlying the Patagonia Formation is the Rodados Patagónicos (Patagonian Boulders) representing a fluvioglacial lithostratigraphic unit of Quaternary age. It has a large areal extent and continuity, and is generally subdivided at various levels. This unit is characterized by a variable thickness, usually between 8 m and 10 m, increasing slightly as it covers paleochannels carved on the surface of Patagonian erosion. The Rodados Patagónicos are made up of different gravel size sand range from rounded to subrounded, and also contains sand, and a

Fig. 2 Hydrogeological scheme of study area showing major geochemical reactions, regional groundwater flow, and various hydrostratigraphic units

scarce silt–clay matrix. The boulder unit matrix is generally loose except for the top of the section which has carbonate cements.

Geomorphology

The study area is part of the plateau relief known as Pampa del Castillo, above 650 m height, which is sub-horizontal and has a smooth NE slope of the order of 0.2–0.3%. The typical landscape of the region is usually crowned in basalts, competent strata of the Patagonia Formation or the Rodados Patagónicos lithological unit. The topography in the SE area of the Pampa del Castillo is characterized by an irregular relief, due to the existence of numerous valleys oriented from west to east, known locally as canyons. These are the product of fluvial erosion in the Upper Pleistocene (Isla et al. 2015) when the climate was much wetter than today. The main canyons are spread over some 10 km, down from 700 to 500 m to as low as 150 m, with slopes between 2 and 3%. The difference in height between the valleys and interfluves is about 200 m and the width of valleys is between 2 and 4 km. These valleys are currently dry, but it is clear that in the past, they were carved by rivers that originated from rainfall much greater than modern streams in the region. Thus, the abrupt change in slope between the plateau relief and canyons occurs between 650 and 700 m. Surface water erosion and mass removal processes occupy the interfluves and heads of canyons. The alluvium, generally thin, is located in stream beds in the valleys, and pediments represent surfaces of erosion with scarcely any significant slopes.

Because of the inversion of the relief, they constitute plateaus which in the central sector of the Santa Cruz Province are dissected by the valley of the Seco River (Fig. 1) and other ephemeral streams forming canyons (Hernández et al. 2008). These landforms exercise significant control on the subsurface hydrodynamics, since the superficial divide coincides with the subterranean one, and the canyons constitute the areas of natural discharge of groundwater. Other discharge sites are natural springs, which generally coincide with the contact between sandy and mudstone sections of the Patagonia Formation.

Hydrogeology

There exist few hydro-geological background investigations as has been referred to in the study area. The total depth of most of the water wells reaches mudstone sequences of the Patagonia, Sarmiento and Río Chico formations, and in some cases, the screened section is entirely within these levels (CFI 1992). Hernández and Hernández (2013) assigned the study area to a specific hydrogeological pattern dominated by the León Canyon Pattern, characterized by sandy components dominating in the Patagonia Formation and generally overlying an aquiclude corresponding to the tuffs of the Sarmiento Formation.

The hydrogeological basement consists of the top of the Río Chico Formation, composed of clays of Paleocene age. Above this basement, the Patagonia Formation contains two aquifers, the lower one confined and the upper one, semi-confined, being separated by a clay layer 8–10-m thick.

Finally, the Rodados Patagónicos lithological unit forms an unconfined aquifer (Fig. 2). For the semi-confined aquifer, the recharge is indigenous, directly through this sequence, where temporary retention occurs. The groundwater level depth is 5 m or less for the phreatic aquifer and 30 m for the semi-confined one. Permeabilities are between 50 and 1 m/day for the Rodados Patagónicos unit, depending on the percentage of carbonate cement. A relatively low hydraulic conductivity of 2×10^{-2} m/day in contrast is characteristic of the aquifer located at the top of the Patagonia Formation. The confined aquifer recharge comes from the allochthonous contribution taking place at the sandy outcrops of the western Patagonian (the Seventy Pampa near the town of Las Heras: 46°33′S, 68°57′W), which defines a south to east direction of the groundwater flow. Groundwater levels are between 65- and 70-m deep and the established hydraulic conductivity is between 0.5 and 1 m/day.

The water extraction in the area is conducted via four sets of wells: three in the Espinosa Plateau and one in the Quintar Canyon (Fig. 1). The water system includes 56 deep boreholes in total. The oldest set is located in Quintar Canyon, with 32 wells still in service, despite 29 of them having some kind of operational problem due to construction mode, design, or chemical quality. On the plateau, the sets of wells extract water in the semi-confined and confined aquifers between 110- and 200-m depths, respectively. Pumping and recovery tests performed allow an overall estimation of aquifer parameters for the confined aquifer of a transmissivity (T) of 25 m^2/day and a storage coefficient (S) of 4×10^{-4}. For the semi-confined aquifer, T values obtained vary between 70 and 115 m^2/day, and S values range from 3×10^{-3} to 4×10^{-4}. Furthermore, typical flow rates measured for the confined and semi-confined aquifers were 0.5 and 1 m^3/h per meter of aquifer drawdown, respectively.

The entire study area exploits the same aquifer formations; these areas are receiving indigenous contributions and allochthonous water. In the set of wells of the Quintar Canyon site, the Rodados Patagónicos unit disappears, with a difference in elevation between this set and the plateau of 108.5 m (CFI 1987a, 1991). At this location, the semi-confined aquifer acquires an unconfined status due to the disappearance of the clay in the distal part of the canyon (CFI 1987a, b, 1991, 1992).

Materials and methods

Data collection

A database including 1756 chemical analyses (1998–2002) realized in the three Espinosa Plateau set of wells and in the Quintar Canyon from the Public Water Supply Company was used. Chemical analyses include major ion composition through standard methods and were performed following detailed methodology in APHA (1995). Chloride (Cl^-) concentrations were measured following the Mohr method, sulfate (SO_4^{2-}) by turbidimetry, calcium (Ca^{2+}) and magnesium (Mg^{2+}) by complexometric titrations with EDTA. Sodium (Na^+) and potassium (K^+) concentrations were determined by flame spectrometry, and bicarbonate (HCO_3^-) by potentiometric titration.

Statistical analyses

After applying criteria of electroneutrality to accept or reject records, a final number of 193 data were utilized for this work. These are distributed in the studied sets as follows (Fig. 1):

1. Quintar Canyon (QC): a total of 120 samples were analyzed.
2. Espinosa Plateau I (EPI): a total of 30 samples were analyzed.
3. Espinosa Plateau II (EPII): a total of 34 samples were analyzed.
4. Espinosa Plateau III (EPIII): a total of nine samples were analyzed.

Through the geological knowledge of the area, it should be expected that each studied area (QC and EP I, II and III) reflects unique chemical characteristics. Such geochemical signatures are most probably the result of the geological and climatic variables, and the carbon dioxide partial pressures (P_{CO2}) values mainly as soil gases. Once a linkage is determined between the study area earth materials and circulating waters, it may be possible to differentiate distinct physicochemical characteristics. These characteristics may or may not correlate well with the number of existing wells. The goal of this study is to objectively identify physicochemically distinct groundwaters relative to given sets of wells. This requires performing statistical analysis of water wells. The analysis was conducted at two levels: first on an exploration level, and secondly, on an analytical and validation level. Both are described below:

Exploration

For each area under study (QC and EP I, II and III), measures of central tendency (arithmetic mean and median) were analyzed. The results of minimum, median, variances, maximum, outliers and extreme values were displayed in box plots for each variable discriminated per a given set, which enables visualization of the data distribution.

Statistical model and validation

The proposed model assumes that the effect of each treatment (tj) acts in a homogeneous way in all units of analysis:

$$y_{ij} = \mu_j + t_j + e_{ij},$$

y_{ij}: population mean, $t_j = \mu_i - \mu$: effect of the treatment, e_{ij}: random component.

The random term e_{ij} (experimental error) represents the variability. The statistical techniques require the validation of the model. In this case, the existence of homoscedasticity of variance and normality of the data need to be confirmed (Mandel 1969). The validation of the normality of the data was performed using the Kolmogorov–Smirnov test, with a p value of 0.05 established to accept or reject the hypothesis $H0$ of data normality.

The homoscedasticity of variances was tested with the Levene test, with a p value of 0.05 established to accept or reject the hypothesis $H0$ of equality of variances. This test was used because it provides good robustness against non-normal data. It is defined as:

$$H0: \sigma 21 = \sigma 22 = \cdots = \sigma 2k.$$

$$H1: \sigma 2i \neq \sigma 2j; \quad \text{for at least one pair (imp)}$$

The analysis of homoscedasticity of variance was necessary to define the application of a parametric or non-parametric test upon an analysis of mean comparison. Non-parametric methods are useful when the assumption of normality is not met, but it is essential to assume that the observations of the samples are independent and arise from the same distribution. In addition, in the designs of two samples, the assumption of equality of form and dispersion is required. The hypotheses for the non-parametric method are:

$$H0: \mu = \mu 0.$$

$$H1: \mu \neq \mu 0.$$

For the analysis, the Kolmogorov–Smirnov test is also used to assess the independence among samples (Perez 2003).

General hydrogeochemistry

The physico-chemical analyses results determined by the state laboratory allow characterizing groundwater, and piper diagrams were used to describe the hydro-chemical composition of groundwater. The PHREEQC software (Parkhurst and Appelo 1999) was used for the calculation of all speciation and saturation indexes (SI) and P_{CO2} values, as well as for performing hydrochemical modeling.

Results

Statistical analysis

The statistical tests were conducted to demonstrate whether or not major ions of each set, Quintar Canyon (QC), Espinosa Plateau I (EPI), Espinosa Plateau (EPII) and Espinosa Plateau III (EPIII) could be clustered under a single population that in turn, could be linked to the set name where these waters originated. This was accomplished by applying the criteria associated with the exploration and validation analyses mentioned above.

Exploration

The hydrochemical composition of groundwater can be characterized from the statistical parameters of the distribution of values for each ion relative to each operation area (Table 1). When box plots are analyzed (Fig. 3), it can be seen that the median varies in a stepwise manner in the transect from EPIII to CQ, with values being apparently similar in EPI and EPII. As can be seen in Fig. 3, differences between the medians of the major ions and electrical conductivity (EC) can be observed. When the median values of the discharge area (QC) and the rest of the study sites are compared, it can be observed that the ion concentrations and EC values are higher in this set than in the others. Mg^{2+} shows the most dispersion of all cations (Fig. 3d). In QC, the SO_4^{2-} anion highlights the highest outliers' concentrations of the well sets (Fig. 3g). The HCO_3^- median value shows an inverse variation compared to other ions, with a decrease towards the discharge area (QC) or to the east portion of the study area (Fig. 3f). In all box plots, concentrations of all ions do not seem to present significant differences between EPI and EPII, and the median varies in a staggered way in a transect from EPIII to QC. It is also observable that the ions and EC median values are higher in the QC battery and that only HCO_3^- presents a different behavior.

This exploratory analysis suggests that there are no differences between EPI and EPII, which probably would indicate that this is a single set that responds more to an administrative division than to a hydrochemistry one. Furthermore, both EPI and EPII are located in essentially identical longitudinal positions, have similar hydrostratigraphy and are positioned at similar locations of the hydrologic gradient. From the analysis of the box plots, it can be inferred that there are differences between the median values of the well sets analyzed and, in addition, an ion's concentrations increment is reflected in the east direction, with the exception of HCO_3^- that increases in the opposite direction.

Table 1 Descriptive statistics for each battery under study

Battery	Parameter										
	Descriptive statistics	EC	T	TDS	Na^+	Ca^{2+}	Mg^{2+}	Cl^-	HCO_3^-	SO_4^{2-}	P_{CO2}	Ca/Mg
		μS/cm	°C	mg/L							atm	mmol/L
EPIII	Mean	875	20.7	524	159.6	14.6	8.0	97.3	245.9	82.3	− 2.94	1.2
	Median	860	20	510	149.5	14.4	7.2	96	236.7	86.4	− 2.94	1.1
	SD	106	1.1	46.9	28.7	3.3	2.2	12.5	29	25.0	0.04	0.3
	Asymmetry	0.17	0.8	− 0.3	1.8	1.17	1.7	0.5	1.6	− 0.02	0.23	0.3
	Kurtosis	0.06	− 1.7	− 0.8	2.9	1.6	2.9	− 0.7	2.3	− 1.5	− 4.34	1.5
	Minimum	701	19.7	444	138	10.9	6.2	80	219.6	48.3	− 2.97	0.8
	Maximum	1050	22.2	582	224.3	21.6	13.0	116	310.0	112.0	− 2.90	1.6
EPI	Mean	1056	19.9	713	201.3	19.7	13.9	170.5	179.5	164.4	− 2.97	0.9
	Median	1050	20.2	706	201.3	20	11.7	164	175.7	152.4	− 2.99	0.9
	SD	145.8	1.54	72.4	201.1	4.5	5.2	26.5	23.1	67.2	0.06	0.1
	Asymmetry	0.72	− 0.08	0.72	− 0.3	0.37	1.7	0.55	0.56	1.3	1.20	0.8
	Kurtosis	0.52	0.45	− 0.08	− 0.1	− 0.43	2.9	− 0.8	− 0.43	2.0	0.14	0.7
	Minimum	821	17.2	613	115	12.8	7.7	132	144.0	66.0	− 3.04	0.7
	Maximum	1450	23.1	899	259	30.5	30.7	222	231.8	363.3	− 2.86	1.2
EPII	Mean	1158	26.2	706	228.7	18.3	14.7	179.8	196.1	164.7	− 3.08	0.8
	Median	1123	20	773	221.3	17.2	13.5	193	194	169.6	− 3.05	0.8
	SD	253.5	34.8	134.8	71.3	4.7	7.5	52.9	36.8	46.6	0.11	0.1
	Asymmetry	322	5.8	− 0.2	1.0	0.4	1.9	− 0.2	0.4	− 0.3	− 1.95	− 0.3
	Kurtosis	− 1.09	34	− 1.7	0.8	− 0.9	3.8	− 1.6	0.4	− 0.9	− 2.18	− 1.1
	Minimum	772	17.6	505	126.5	11.3	7.2	100	122	74	− 3.36	0.6
	Maximum	1600	223	886	414	28.9	40.7	254	295.2	234.4	− 2.95	0.9
QC	Mean	1837	20.2	1191	366.1	29.0	18.1	343.1	161.1	302.4	− 2.94	1.0
	Median	1850	20.4	1189	364.1	29.5	17.3	337	158.6	304.8	− 2.97	1.0
	SD	512	1.9	294.2	122.6	6.8	5.7	116.5	36.1	91.7	0.12	0.2
	Asymmetry	0.2	− 1.9	− 0.2	0.5	0.1	1.1	0.3	1.2	− 0.5	0.57	0.2
	Kurtosis	0.4	5.0	− 0.05	0.4	− 0.2	2.6	− 0.1	2.4	0.6	0.35	0.2
	Minimum	660	13.6	460	108.1	14.4	8.6	102	100.0	24.5	− 3.17	0.6
	Maximum	3400	23.1	1827	770.5	49.7	43.6	650	302.6	496.6	− 2.68	1.3

SD standard deviation, *EC* electrical conductivity, *T* temperature, *TDS* total dissolved solids, P_{CO2} CO_2 partial pressure

## Statistical model and validation

To statically check the observed chemical similitudes and differences among the exploitation sectors, statistical tests were performed. Initially, the hypothesis of normality of the data was tested using the correction of Lilliefors (Table 2). For EC and Ca^{2+}, the results showed acceptance of the hypothesis $H0$ of normality of the data, which was met at a p value of 0.05. However, the rest of the ions and well sets partially verify the hypothesis of normality of the data.

According to the assumptions of the statistical model (homoscedasticity of variances), the proper use of parametric methods can only be allowed in some cases (Table 3). When the homoscedasticity of variances could not be assumed, a non-parametric test for mean comparison was used. From this analysis, it is showed that there are no significant differences between EPI and EPII, confirming what was observed in the exploratory analysis, except for Cl^-. Comparing EPII and EPIII, Ca^{2+} is the only element that shows equality between means (Table 4).

The exploratory analysis allowed deducing that differences between EPI and EPII are negligible. The confirmatory analysis agrees with this result; however, Cl^- falls in the rejection region of the hypothesis of equality of means. Despite this result, it can be concluded that EPI and EPII could be considered as the same water for practical purposes. In this way, three different groups are determined from the point of view of major ions: EPIII, EPI–EPII and QC.

Fig. 3 Box plots for the set of wells under study: QC and EP I, II and III. Circles and asterisks represent outliers and extreme values, respectively
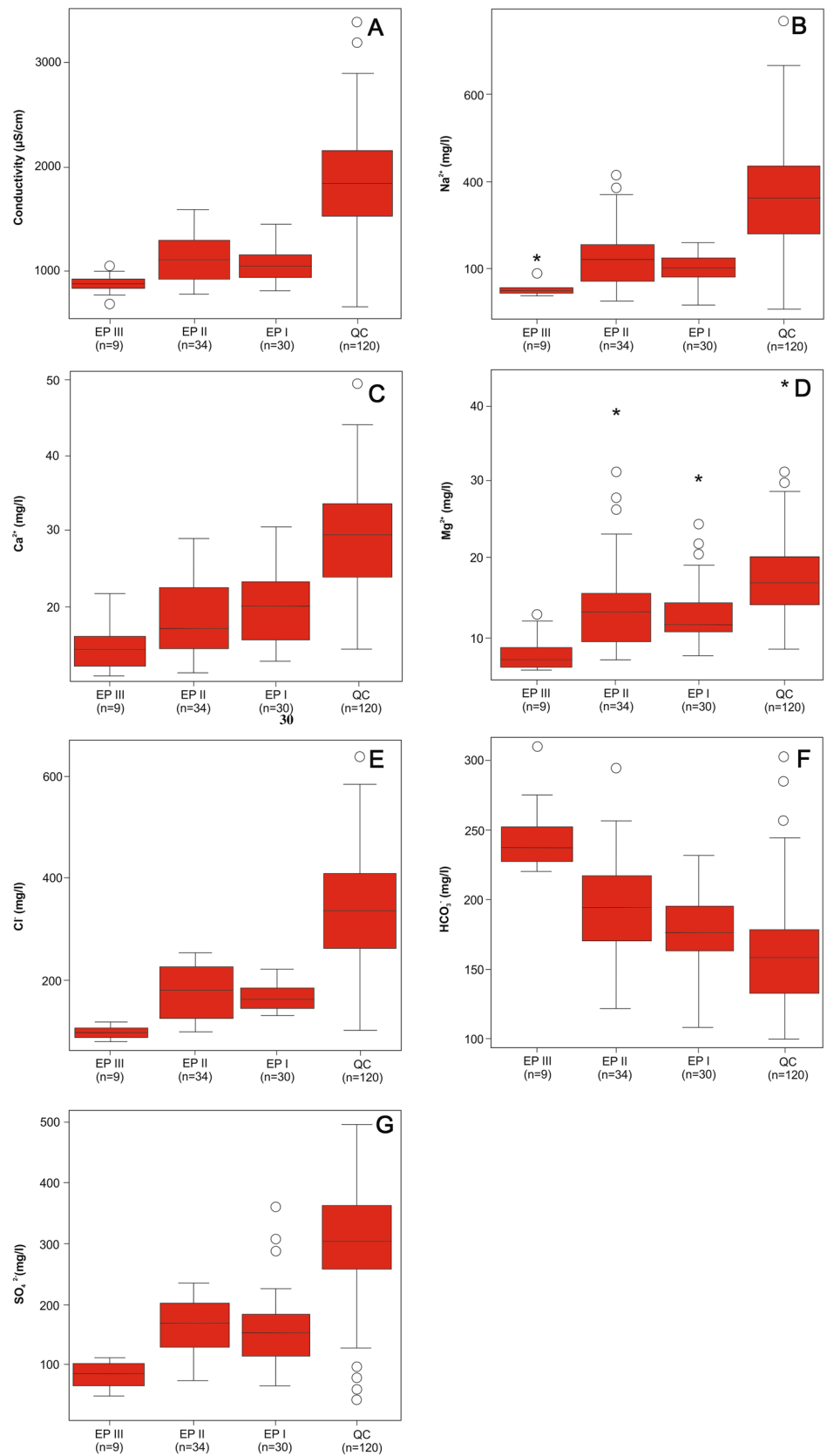
Table 2 Test of data normality—Test of Kolmogorov–Smirnov

Parameter	Level of significance (p value) Study area				Conclusion
	EPIII	EPII	EPI	QC	
EC	0.200[a]	0.065	0.061	0.200[a]	$H0$ accepted for all data
Na^+	0.200[a]	0.200[a]	0.026	0.004	$H0$ accepted for the data of QC and EPI, and rejected for EPII and EPIII
Ca^{2+}	0.097	0.200[a]	0.200[a]	0.200[a]	$H0$ accepted for all data
Mg^{2+}	0.020	0.000	0.001	0.200[a]	$H0$ accepted for the data of QC, EPI and EPIII, and rejected for EPII
Cl^-	0.200[a]	0.150	0.002	0.200[a]	
HCO_3^-	0.001	0.098	0.175	0.083	$H0$ accepted for the data of EPI, EPII and EPIII, and rejected for QC
SO_4^{2-}	0.014	0.046	0.200[a]	0.200[a]	$H0$ accepted for the data of EPII and EPIII, and rejected for EPI and QC

[a]Correction of Lilliefors

Table 3 Test of homoscedasticity of variances—Test of Levene

Study area	Level of significance (p value) Ion						Conclusion
	Na^+	Ca^{2+}	Mg^{2+}	Cl^-	HCO_3^-	SO_4^{2-}	
QC/EPI	0.000	0.009	0.500	0.000	0.086	0.091	$H0$ accepted for Mg^{2+}, HCO_3^- and SO_4^{2-}
QC/EPII	0.001	0.029	0.246	0.001	0.736	0.005	$H0$ accepted for Mg^{2+} and HCO_3^-
QC/EPIII	0.003	0.018	0.034	0.001	0.529	0.022	$H0$ accepted for HCO_3^-
EPI/EPII	0.017	0.475	0.214	0.000	0.051	0.280	$H0$ accepted for Ca^{2+}, Mg^{2+}, HCO_3^- and SO_4^{2-}
EPI/EPIII	0.381	0.221	0.080	0.016	0.616	0.091	$H0$ accepted for all ions, except Cl^-
EPII/EPIII	0.066	0.063	0.054	0.000	0.420	0.062	

Table 4 Non-parametric test of means comparisons—Test of Levene

Study area	Level of significance (p value) Ion						Conclusion
	Na^+	Ca^{2+}	Mg^{2+}	Cl^-	HCO_3^-	SO_4^{2-}	
QC/EPI	0.000	0.000	0.000	0.000	0.007	0.000	$H0$ rejected for all ions
QC/EPII	0.000	0.000	0.000	0.000	0.000	0.000	
QC/EPIII	0.000	0.000	0.000	0.000	0.000	0.000	
EPI/EPII	0.163	0.598	0.382	0.049	0.087	0.625	$H0$ accepted for all ions, except Cl^-
EPI/EPIII	0.014	0.003	0.028	0.000	0.000	0.000	$H0$ rejected for all ions
EPII/EPIII	0.007	0.216	0.002	0.000	0.000	0.000	$H0$ accepted for Ca^{2+} and rejected for all other ions

General hydrochemistry

The representation of the ionic composition in piper diagrams (Fig. 4) shows a general predominance of sodium waters in all sectors. Nevertheless, an evolutionary trend in the anion composition of the water can be observed due to the increasing of chloride from the EPI to the QC.

Distribution of elements and hydrogeochemical evolution

The regional direction of the groundwater flow is from west to east, with the plateau being the recharge (EPIII) and transit (EPI and EPII) areas and the canyon (QC) the discharge area. The geographical distribution of the major elements
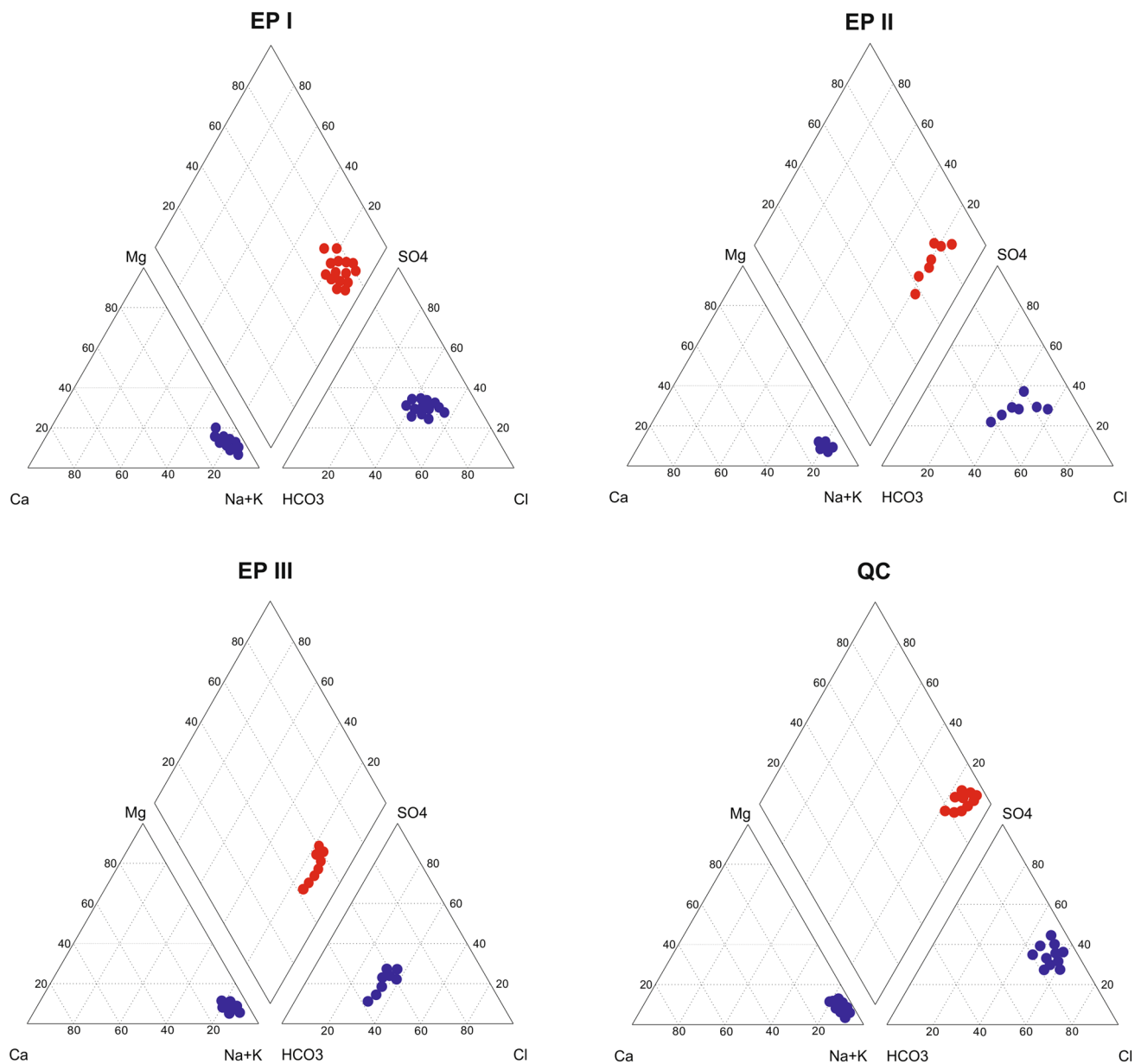
Fig. 4 Piper diagrams showing the ionic composition of groundwater in the study area

shows an incremental increase of EC and Na^+, Ca^{2+}, Mg^{2+}, Cl^- and SO_4^{2-}, and a decrement of HCO_3^- in the flow direction. The EC average value increases from 875 to 1837 μS/cm, similarly in the groundwater flow direction toward QC. The minimum values correspond to the wells of the Espinosa Plateau sets, while the highest ones, with a maximum of 3400 μS/cm, are characteristics of the Quintar Canyon set (Fig. 5). Cl^- and SO_4^{2-} increase almost in the same proportions in the same direction, and Na^+ follows the same pattern and rises from mean values of 159.6 to 366.1 mg/L. The Ca^{2+} and Mg^{2+} concentrations' increase also has a similar pattern, with a range of average values varying between 8.0

and 29.0 mg/L. The Ca/Mg ratio (in mmol/L) remains constant around 1.0 throughout the area. The only major ion that decreases in the flow direction is HCO_3^-, from 245.9 to 161.1 mg/L in the discharge area, the QC area (Table 1).

For the reactive mineral phases identified in the geological formations of the aquifer system under study (calcite, dolomite and gypsum), saturation indices (SI) were calculated in wells including field data of temperature and pH (Table 5) and the mean SI for each set of wells are represented in Fig. 6. Calcite is close to equilibrium, with SI values varying between − 0.23 and 0.38 (Table 5). Dolomite SI values, of between − 1.87 and 0.97 (Table 5), show a slight
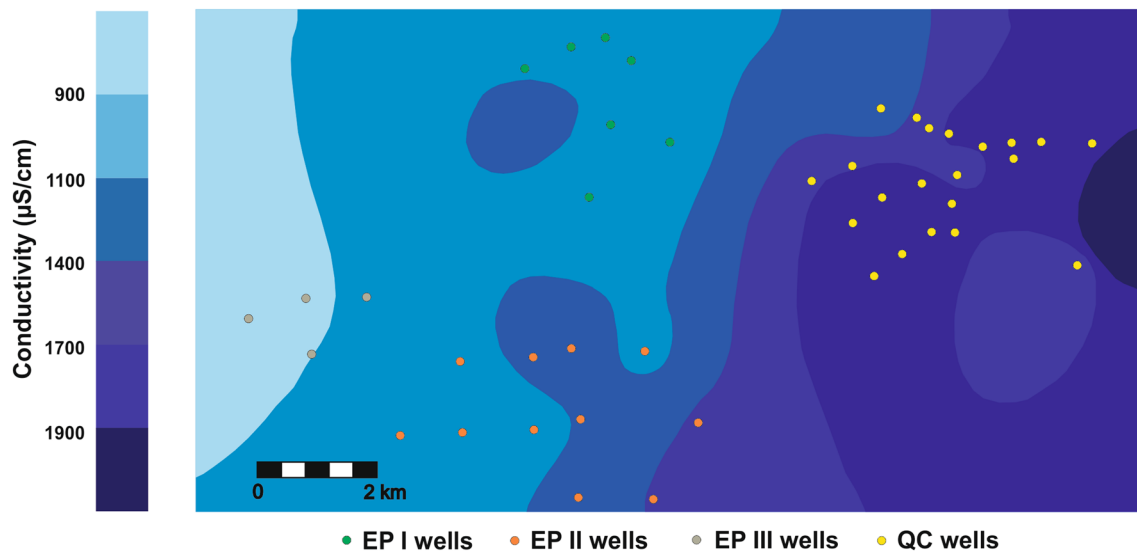
Fig. 5 Electrical conductivity (µS/cm) evolution along the EPIII-QC transect

Discussion

The hydrogeochemical evolution of the aquifer, from EPIII to QC, shows a general augmentation of EC and major ions, except for HCO_3^-. Piper diagrams display that waters are sodium type in all groundwater systems, and become gradually more sulfated and chlorinated in the flow direction, following a normal hydrochemical evolution (Chebotarev 1955). As already mentioned, the only ion whose concentration decreases is HCO_3^-.

Figure 7 shows the Na^+ vs. Cl^- ratio. The samples are in a line with a slope lower than the line corresponding to the halite dissolution process (1:1), indicating an excess of Na^+ with respect to its possible origin. On the other hand, the observed Na/Cl ratio, represented by a line slope of 0.68, is closer to the seawater ratio (0.86), indicating that the source of both ions is the seawater aerosols in precipitation. Regardless, a decrease in the Na^+ content is commonly caused by a process of ion exchange with Ca^{2+}. The Ca^{2+} in solution exchanged with the Na^+ released may be provided by the dissolution of gypsum of the Patagonia Formation. The solubility of gypsum is supported by the existence of undersaturated conditions with respect to gypsum throughout the study area.

The increase of SO_4^{2-} towards the discharge area results from the dissolution of gypsum, and it is only partially

supersaturation in the western area (EPII and EPII), and then reach equilibrium conditions toward the QC area (Fig. 6). Finally, gypsum is undersaturated in the entire study area, but with SI values increasing from −2.51 in the western area to −1.24 at the QC site (Table 5).

accompanied by an augmentation of Ca^{2+}. Besides the exchange of Na^+, Ca^{2+} concentration in ionic solution is controlled by the precipitation of calcite in equilibrium conditions throughout the area. This process also explains the decrease of HCO_3^- in the flow direction (Figs. 3f, 8).

This process of dissolution of gypsum with calcite precipitation, leading to a decrease in HCO_3^- concentration, has a consequence on the dolomite SI values. Indeed, the saturation of dolomite goes from supersaturated in EPII and EPIII, to close to equilibrium conditions in the EPI and QC area. This dolomite dissolution is associated with the process of dedolomitization. Such reactions have been well studied in the Madison aquifer (USA) (Plummer et al. 1990), the East Midlands Triassic sandstone (UK) (Edmunds et al. 1982), the Turonian aquifer [Tunisia; (Abid et al. 2011)]. The dedolomization process has also been described in Deike (1990), Bischoff et al. (1994), Raines and Dewers (1997), Stoakes et al. (2014) and Thirathititham and Whitaker (2017).

The dedolomitization occurs according to the Eq. (1), (after Appelo and Postma 1999):

$$1.8\ CaSO_4 + 0.8\ CaMg(CO_3)_2 \rightarrow 1.6\ CaCO_3 + Ca^{2+} + 0.8Mg^{2+} + 1.8\ SO_4^{2-}. \tag{1}$$
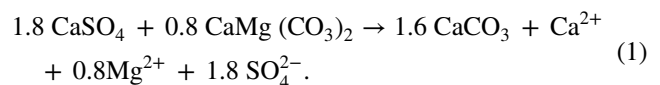
From this equation, a good correlation among Ca^{2+} vs. SO_4^{2-} and Ca^{2+} vs. Mg^{2+} is expected. This correlation can be shown through a graph including the samples of the study wells. A linear relationship in the increase of Ca^{2+} and SO_4^{2-} is observed. A linear increase, but with a lower slope, is also observed for Ca^{2+} vs. Mg^{2+}. On the other hand, a decreasing trend can be seen for HCO_3^- vs. Ca^{2+}, which is the result of the calcium carbonate precipitation (Fig. 8). Dolomite is present as cement both in the Patagonia

Table 5 Saturation indexes (SI) of calcite, dolomite and gypsum calculated using PHREEQC software for each well under study and descriptive statistics

Battery	Well number	SI		
		Calcite	Dolomite	Gypsum
EPIII	24	0.18	0.37	−2.21
	25	0.22	0.46	−2.27
	26	0.22	0.63	−2.51
	27	0.32	0.52	−2.41
EPI	2	−0.01	0.15	−2.03
	3	0.05	−1.87	−1.87
	4	0.10	0.33	−2.17
	6	0.02	0.11	−1.86
	7	0.01	0.09	−2.21
	8	0.13	0.24	−2.00
	9	−0.06	0.14	−2.14
	10	0.14	0.37	−1.90
	11	0.06	0.28	−2.11
EPII	12	0.20	0.67	−2.07
	13	0.21	0.54	−2.21
	14	0.23	0.68	−2.37
	15	0.23	0.55	−2.02
	16	0.17	0.50	−1.86
	17	0.12	0.40	−1.88
	18	0.14	0.39	−1.80
	20	0.38	0.97	−2.11
	21	0.06	0.37	−2.16
	22	0.21	0.53	−2.00
	23	0.14	0.46	−2.45
QC	1	−0.11	−0.11	−1.74
	2	−0.02	0.08	−1.76
	4	−0.10	−0.12	−1.65
	5	−0.23	−0.44	−1.55
	7	−0.07	−0.06	−1.61
	8	−0.04	0.05	−1.80
	9	−0.08	0.04	−1.87
	10	−0.14	−0.16	−1.78
	11	0.38	0.89	−1.67
	12	0.17	0.54	−1.72
	13	−0.13	−0.12	−1.86
	14	−0.03	0.01	−1.74
	15	−0.07	−0.22	−1.61
	16	−0.04	−0.02	−1.76
	17	−0.03	−0.06	−1.58
	18	−0.01	0.02	−1.55
	19	0.06	0.16	−1.53
	20	0.29	0.62	−1.24

Table 5 (continued)

Battery	Well number	SI		
		Calcite	Dolomite	Gypsum
	21	0.03	0.27	−1.75
	22	0.06	0.15	−1.54
	23	0.15	0.38	−1.64
	26	0.34	0.70	−2.23
	31	0.10	0.13	−1.68
	32	0.01	0.07	−1.78
Mean		0.08	0.22	−1.90
Median		0.06	0.26	−1.86
Standard deviation		0.14	0.43	0.28
Asymmetry		0.18	−2.32	−0.24
Kurtosis		−0.52	10.79	−0.40
Minimum		−0.23	−1.87	−2.51
Maximum		0.38	0.97	−1.24

Formation and in the Rodados Patagónicos lithological unit. There are some studies, in the Chubut and Neuquén Provinces (where the cement of the Rodados Patagónicos sequence is described (Martinez and Kutschker 2011). In the Province of Chubut, a study was carried out by the CENPAT (National Patagonian Center, National Council of Scientific and Technical Research—CONICET) on the eastern edge to the limit with the Santa Cruz Province. This work mentions the existence of calcite, dolomite and gypsum, with a predominance of calcium carbonate in the Rodados Patagónicos' cement (Del Valle and Beltramone 1987). On the other hand, in the Province of Neuquén, magnesium calcite presence has been cited (Tunik et al. 2009). As mentioned previously, dolomite is present as cement in both the Patagonia Formation and the Rodados Patagónicos lithological unit. Accordingly, cement composed of carbonates such as calcite, magnesium calcite or dolomite would provide ions such as Ca^{2+}, Mg^{2+} and CO_3^{2-}. These ions being incorporated into the aquifer depend on the degree of the cement solubility, vertical permeability, facies changes, etc. The Rodados Patagónicos unit is present on the top of the plateaus, but has been eroded and dissected in the canyons where it is now eroded away. The recharge of the Patagonia Formation is then by direct infiltration in the canyons, and dripping from the Rodados Patagónicos in the plateaus.

To check this conceptual model, hydrochemical modeling using PHREEQC software was carried out. Direct models were performed simulating the composition resulting from the reaction of hypothetical rainwater with carbonate cements, under closed or opened systems to CO_2, and considering different values of P_{CO2} (Fig. 9). As an example, for the observed values of dissolved Ca^{2+} in the EPIII set,
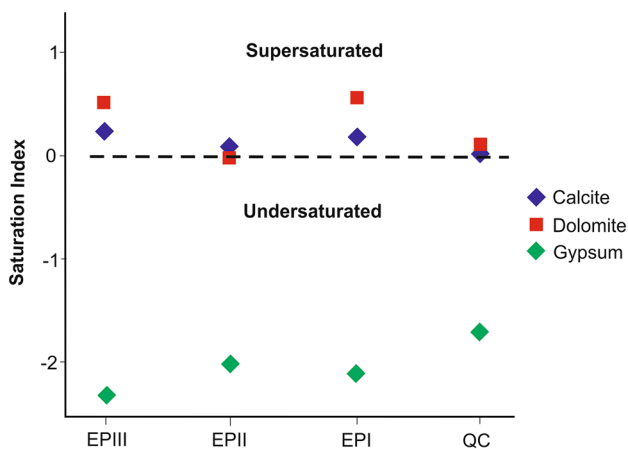
Fig. 6 Saturation indexes of calcite, dolomite and gypsum calculated using PHREEQC software for each area under study
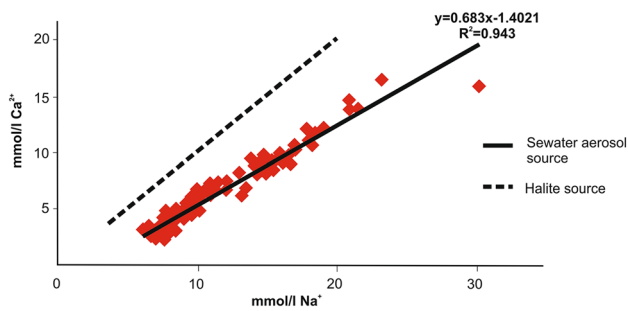
Fig. 7 Na^+ vs. Cl^- (mmol/L) for all wells under study

a better fit to the modeled values was obtained when the dissolution of dolomite cement in an open system is considered. This is due to the fact that the recharge in the plateau area occurs through the Rodados Patagónicos unit, with the aquifer being actually semi-confined and therefore, the two

units behave as a single aquifer system. The reaction begins in this unit and rainwater later reaches the exploited aquifer via vertical infiltration, resulting in the observed geochemistry (Fig. 9). On the other side, in the canyon, where the Rodados Patagónicos unit is not present and water infiltrates directly into the Patagonia Formation, it is difficult to find adjustments in order to explain the dissolved calcium concentration in the area considering just the reactivity with carbonates.

Alternatively, to identify main geochemical processes in groundwater evolution of the transect from EPIII to QC, two inverse models were conducted (Table 6), accepting an analytical error of 5% and using the water mean composition for each set of wells considered either as the initial or final solution. In each set of initial and final solutions, 4–8 possible models were obtained, namely those possessing most of the observed mineral phases. For this analysis, models have been selected including the following components: calcite, dolomite, gypsum, halite, $CO_{2(g)}$ and ionic exchange of Ca^{2+}, Mg^{2+} and Na^+. These reactant processes were selected because of: (1) a CO_2 open system can be assumed from the unconfined condition of the aquifer formed in the Rodados Patagónicos unit present on the plateau area, and the aquifer contained in the upper section of the Patagonia Formation in the canyon area, where the Rodados Patagónicos unit disappears; (2) the sediments' texture includes clay-size particles, which provokes higher exchange capacity; (3) the presence of gypsum, dolomite and calcite in the cement composition of the geological units under study; and (4) the previous investigations performed in the area.

Halite is not present in the aquifer's matrix, but the source of Na^+ and Cl^- is from seawater aerosols present in rainwater that is recharging this hydrological system; however, its dissolution process is included to explain the increase of Na^+ and Cl^- concentrations in the flow direction, from west to east.

Fig. 8 Ca^{2+} vs. SO_4^{2-}, HCO_3^- and Mg^{2+} (mmol/L) for all wells under study
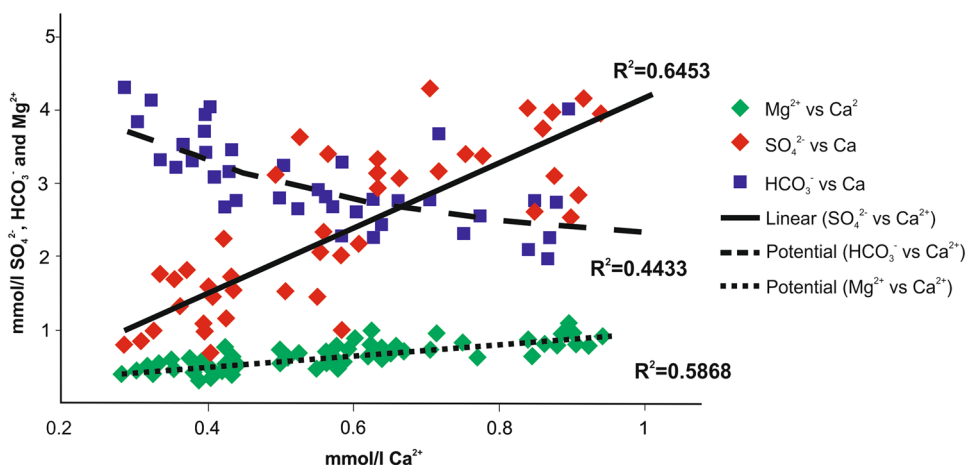
Fig. 9 Modeled vs. observed average calcium values comparison for the EPIII set. Closed and open systems of calcite and dolomite cement dissolution under different values of PCO$_2$ were considered
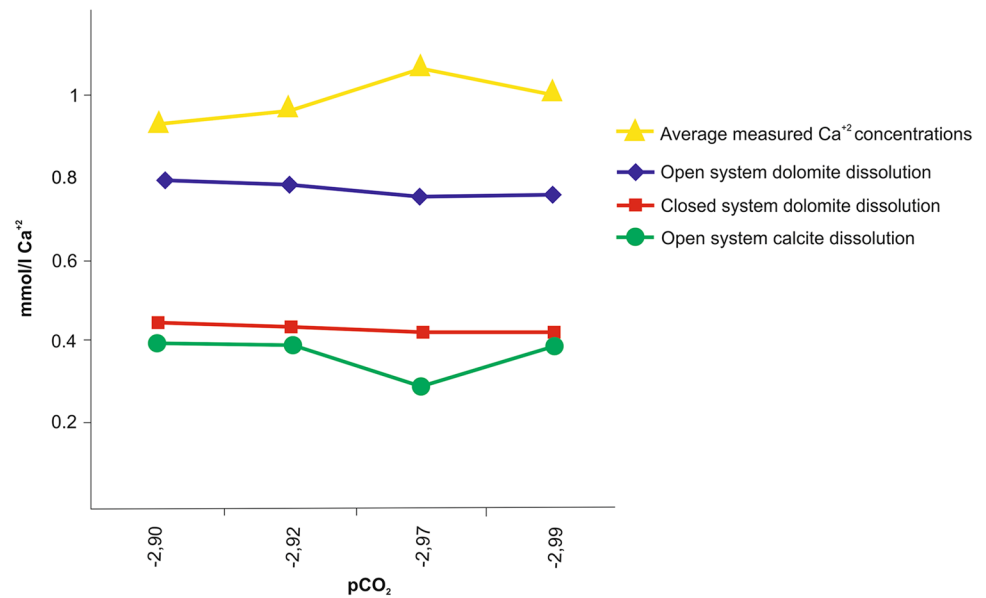
Table 6 Inverse hydrochemical modeling for the EPIII-QC transect

Mineral phase	Model 1		Model 2	
	IS	FS	IS	FS
	EPIII	EPI–EPII		QC
Calcite	− 1.03		− 0.50	
Dolomite	0.24		0.17	
Gypsum	0.85		1.44	
Halite	2.07		4.88	
CO$_{2(g)}$	− 0.55		− 0.12	
CaX$_2$	0.06		− 0.88	
NaX	− 0.12		1.77	

Reactant phase's values (mmol/L) obtained as result in PHREEQC software outputs

IS initial solution, *FS* final solution

In the first model run, the groundwater average composition of the EPIII set (recharge area) was taken as the initial solution, while the groundwater mean composition of the EPI battery (in representation of the EPI–EPII transition area) was the final one. In the second model performed, the latter was used as the initial solution, whilst the groundwater average composition of the QC set (discharge area) was the final one. For these two models, the considered results show that gypsum dissolution with calcite precipitation, Ca^{2+}/Na$^+$ ionic exchange and dedolomitization are the main processes along the groundwater flow path. As can be observed in Table 6, from EPIII to EPI–EPII, the dissolution of gypsum of the Patagonia Formation's cement carries the calcite precipitation (CO$_{2(g)}$ outgassing) and controls the Na$^+$ content decrease in the plateau area. Na$^+$ is then adsorbed on exchange surfaces while Ca^{2+} is released. In this area, rainwater infiltrates and

dissolves the Rodados Patagónicos unit's cement that contains calcite, magnesium calcite and dolomite. The resulting solution reacts with the gypsum present in the Patagonia Formation and causes dolomite dissolution (dedolomitization), a process that also provides Ca^{2+} (and Mg^{2+}) to the solution.

Towards the canyon area, from EPI–EPII to QC, gypsum continues dissolving in a greater proportion (from 0.85 mmol/L in the first model to 1. 44 mmol/L in the second one). Dolomite dissolution and calcite precipitation reactions decrease (from 0.24 in the first model to 0.17 in the second one, and from 1.03 mmol/L in the first model to 0.50 mmol/L in the second one, respectively), and also Ca^{2+} is adsorbed and Na$^+$ is released. Here, as the Rodados Patagónicos unit's cement disappears, precipitation with lower concentration of Ca^{2+} and Mg^{2+} quickly reaches the aquifer due to a thinner unsaturated area. Furthermore, this region is closer to the Atlantic Ocean and the Rodados Patagónicos unit is not present. As a consequence, the autochthonous recharge water is richer in Na$^+$ and Cl$^-$ions that are coming from aerosols. These chemical characteristics best explain the observed correlation with marine aerosols and the higher proportion of halite dissolution observed in the discharge area (from 2.07 mmol/L in the first model to 4.88 mmol/L in the second one). In this way, although gypsum is still dissolving, the dolomite dissolution and calcite precipitation processes are gradually reduced.

Conclusions

The exploratory and confirmatory statistical analyses of major ions by means of non-parametric methods reflected the existence of three distinct areas: (1) the Plateau Espinosa

III, with the lowest content of total dissolved solids (TDS) (2), one which can be considered a transition area, includes the Espinosa Plateau I and II; and (3) a discharge area, corresponding to the Quintar Canyon (QC). Recharge characteristics are definable in the EPIII set, which is sodium–chloride–bicarbonate type. In contrast, in the down gradient portion of the study area or the QC area, groundwater is predominantly typified as a sodium–sulfate–chloride variety. Between these two types of water, the EPI and EPII fluctuate, behaving as a transition area.

The direct hydrochemical modeling based on the assumptions that: (1) the system is open to CO_2 (2) dolomitic cements are present in EPI, EPII and EPII well sets, and (3) a calcareous cement is present in the QC set, is adequate. Indeed, the results show a good fit between the observed and modeled values. On the other hand, the inverse hydrochemical modeling results strongly suggest gypsum dissolution with calcite precipitation, Ca^{2+}/Na^+ (and Mg^{2+}/Na^+) ionic exchange and dedolomitization being the main processes active along the groundwater flow path.

Silty sands of the Patagonia Formation permit groundwater to flow from the west to the east area and incorporating sulfates via gypsum dissolution. In the Espinosa Plateau area, Ca^{2+}, Mg^{2+}, CO_3^{2-} and probably SO_4^{2-} are added to the solution in the case when precipitation infiltrates through the Rodados Patagónicos unit's cement and dissolves it. The EC analysis marks a general west to south flow direction. In the Quintar Canyon area, the Rodados Patagónicos unit is absent and precipitation, having relatively lower concentrations of Ca^{2+} and Mg^{2+} and higher concentrations of Na^+ and Cl^- (due to the proximity of this area to the Atlantic Ocean), reach the aquifer. Consequently, the dedolomitization reaction, predominant in the plateau, decreases. The water discharge is rich in Na^+, Ca^{2+} Mg^{2+}, Cl^- and SO_4^{2-}, and has a lower alkalinity. Calcite SI values decrease until reaching negative values and this observation allows confirming the gradual reduction of dedolomitization processes. Here, precipitation quickly reaches the aquifer due to the thinner unsaturated area, and in fact, the aquifer reaches the surface in the form of small ponds in some places.

Finally, groundwater is supersaturated with respect to calcite and dolomite in the plateau, and in contrast is undersaturated with both these carbonate minerals in the canyon. This general hydrogeochemical behavior can be expected in most of the groundwater and surface-water systems in the eastern Patagonian landscape. These landscapes are dominated by similar surface and near-surface geology and geomorphic features. This study provides complementary knowledge of the physical environment and hydrological processes in the Santa Cruz Province and should prove to be invaluable for improving water management and for assessing the impact that oil activities may have on precious groundwater resources.

References

Abid K, Zouari K, Dulinski M, Chkir N, Abidi B (2011) Hydrologic and geologic factors controlling groundwater geochemistry in the Turonian aquifer (southern Tunisia). Hydrogeol J 19(2):415–427. https://doi.org/10.1007/s10040-010-0668-z

APHA (1995) WPCF, standard methods for the examination of water and wastewater. American Public Health Association/American Water Works Association/Water Environment Federation, Washington, DC

Appelo C, Postma D (1999) A consistent model for surface complexation on birnessite ($-MnO_2$) and its application to a column experiment. Geochim Cosmochim Acta 63(19–20):3039–3048. https://doi.org/10.1016/S0016-7037(99)00231-8

Auge M, Wetten C, Baudino G, Bonorino G, Gianni R, González N, Grizinik M, Hernández M, Rodríguez J, Sisul A (2010) Hidrogeología de Argentina. Boletín Geológico y Minero 117(1):7–23

Bischoff JL, Juliá R, Shanks WC III, Rosenbauer RJ (1994) Karstification without carbonic acid: bedrock dissolution by gypsum-driven dedolomitization. Geology 22(11):995–998. https://doi.org/10.1130/0091-7613(1994)022%3c0995:KWCABD%3e2.3.CO;2

Boix M, Gigli P (2010) Desafíos comunitarios y recomendaciones. Municipios de Río Gallegos y Caleta Olivia, Santa Cruz. Documento de Trabajo N, 56

CFI. Consejo Federal de Inversiones (1987a) Provisión de agua a Caleta Olivia. Batería de Bombeo Meseta Espinosa 2Informe final

CFI—Consejo Federal de Inversiones (1987b) Provisión de agua potable Las Heras. Estudio del Subalveo del Valle del Rio Deseado. Informe final

CFI—Consejo Federal de Inversiones (1991) Geohidrología del área noreste de la provincia de Santa Cruz. Investigaciones Aplicadas

CFI (1992) Provisión de agua a Caleta Olivia provincia de Santa Cruz. Informe final

Chebotarev I (1955) Metamorphism of natural waters in the crust of weathering—1. Geochim Cosmochim Acta 8(1–2):22–48. https://doi.org/10.1016/0016-7037(55)90015-6

de Barrio R, Panza J, Nullo F (1999) Jurásico y Cretácico del Macizo del Deseado, provincia de Santa Cruz. Geología Argentina 29(17):511–527

Deike RG (1990) Dolomite dissolution rates and possible Holocene dedolomitization of water-bearing units in the Edwards aquifer, south-central Texas. J Hydrol 112(3–4):335–373. https://doi.org/10.1016/0022-1694(90)90023-Q

Del Valle H, Beltramone C (1987) Morfología de las acumulaciones calcáreas en algunos paleosuelos de Patagonia Oriental (Chubut). Ciencia del Suelo 5(1):77–87

Edmunds W, Bath A, Miles D (1982) Hydrochemical evolution of the East Midlands Triassic sandstone aquifer, England. Geochimica et Cosmochimica Acta 46(11):2069–2081. https://doi.org/10.1016/0016-7037(82)90186-7

Feruglio E (1949) Descripción geológica de la Patagonia. In YPF (ed) I–III: Coni Buenos Aires

Hernández L, Hernández MA (2013) Características hidrolitológicas de las formaciones Patagonia y Santa Cruz. Cuenca del Golfo San Jorge. (Provincias de Chubut y Santa Cruz). Agua subterránea recurso estratégico EDULP La Plata 1:112–117

Hernández MA, González N, Hernández L (2008) Late cenozoic geo-hydrology of extra-Andean Patagonia, Argentina. Dev Quat Sci 11:497–509. https://doi.org/10.1016/S1571-0866(07)10024-5

Isla FI, Espinosa M, Iantanos N (2015) Evolution of the Eastern flank of the North Patagonian Ice Field: the deactivation of the Deseado River (Argentina) and the activation of the Baker River (Chile). Zeitschrift für Geomorphologie 59(1):119–131

Lesta PJ (1968) Estratigrafía de la cuenca del Golfo San Jorge. Jornadas Geológicas Argentinas, 3 Actas 1:251–289

Lesta P, Ferello R (1972) Región extraandina de Chubut y norte de Santa Cruz. Geología Regional Argentina 2:602–687

Lhering H (1907) Les mollusques fossiles du Tertiaire et du Crétacé Supérieur de l'Argentine (Vol. Tomo VII: 1–611): Anales del Museo Nacional de Buenos Aires

Mandel J (1969) The partitioning of interaction in analysis of variance. J Res Natl Bur Stand Ser B 73:309–328

Martinez OA, Kutschker A (2011) The 'Rodados Patagónicos' (Patagonian shingle formation) of eastern Patagonia: environmental conditions of gravel sedimentation. Biol J Linn Soc 103(2):336–345. https://doi.org/10.1111/j.1095-8312.2011.01651.x

Parkhurst DL, Appelo C (1999) User's guide to PHREEQC (version 2): a computer program for speciation, batch-reaction, one-dimensional transport, and inverse geochemical calculations. Water-resources investigations report. US Geological Survey, Denver, Colorado, 99-4259

Perez C (2003) Técnicas Estadísticas con SPSS. Ed. Pearson Educación, S.A., Mexico

Plummer LN, Busby JF, Lee RW, Hanshaw BB (1990) Geochemical modeling of the Madison aquifer in parts of Montana, Wyoming, and South Dakota. Water Resour Res 26(9):1981–2014. https://doi.org/10.1029/WR026i009p01981

Raines MA, Dewers TA (1997) Dedolomitization as a driving mechanism for karst generation in Permian Blaine Formation, Southwestern Oklahoma, USA. Carbonates Evaporites 12(1):24–31. https://doi.org/10.1007/BF03175799

Simpson GG (1933) Stratigraphic nomenclature of the early Tertiary of central Patagonia. American Museum novitates, 644

Simpson GG (1935) Occurrence and relationships of the Río Chico fauna of Patagonia. American Museum of Natural History, New York

Stoakes F, Verhoef M, Mahood R (2014) Evolution of a regional interconnected diagenetic aquifer in the lower Prairie Evaporite of northeast Alberta. In: Canadian Society of Petroleum Geologists, 2014 annual meeting, Calgary, Alberta, extended abstract, 2

Sylwan CA (2001) Geology of the Golfo San Jorge Basin, Argentina. J Iber Geol 27:123–157

Thirathititham R, Whitaker F (2017) Charaterising water–rock interaction in a mixed carbonate-evaporite karstified aquifer system, Qatar. In: Paper presented at the AGU fall meeting abstracts

Tunik MA, Pazos PJ, Impiccini A, Lazo D, Aguirre-Urreta MB (2009) Dolomitized tidal cycles in the Agua de la Mula member of the Agrio formation (Lower Cretaceous), Neuquén Basin, Argentina. Latin Am J Sediment Basin Anal 16(1):29–43

WWAP (United Nations World Water Assessment Programme) (2015) The United Nations World water development report 2015: water for a sustainable world. UNESCO, Paris

Zambrano J, Urien C (1970) Geological outline of the basins in Southern Argentina and their continuation off the Atlantic shore. J Geophys Res 75(8):1363–1396. https://doi.org/10.1029/JB075i008p01363